Biosensors and Bioelectronics 213 (2022) 114475

Contents lists available at ScienceDirect

Biosensors and Bioelectronics

journal homepage: www.elsevier.com/locate/bios

Biosensor prototype for rapid detection and quantification of DNase activity

Skomantas Serapinas [a,b,1], Justina Gineitytė [a,c,1], Marius Butkevičius [a,b], Rapolas Danilevičius [b], Marius Dagys [a,c], Dalius Ratautas [a,c,*]

[a] Life Sciences Center, Vilnius University, Saulėtekio al. 7, LT-10257, Vilnius, Lithuania
[b] UAB "Laboratorija 1", Pamėnkalnio g. 36, LT-01114, Vilnius, Lithuania
[c] UAB "Bioanalizės sistemos", Saulėtekio al. 15, LT-10224, Vilnius, Lithuania

ARTICLE INFO

Keywords:
Nuclease
Biosensor
DNA immobilization
DNA hybridization
DNase I

ABSTRACT

DNases are enzymes that cleave phosphodiesteric bonds of deoxyribonucleic acid molecules and are found everywhere in nature, especially in bodily fluids, i.e., saliva, blood, or sweat. Rapid and sensitive detection of DNase activity is highly important for quality control in the pharmaceutical and biotechnology industries. For clinical diagnostics, recent reports indicate that increased DNase activity could be related to various diseases, such as cancers. In this paper, we report a new bioelectronic device for the determination of nuclease activity in various fluids. The system consists of a sensor electrode, a custom design DNA target to maximize the DNase cleavage rate, a signal analysis algorithm, and supporting electronics. The developed sensor enables the determination of DNase activity in the range of 3.4×10^{-4} – 3.0×10^{-2} U mL^{-1} with a limit of detection of up to 3.4×10^{-4} U mL^{-1}. The sensor was tested by measuring nuclease activity in real human saliva samples and found to demonstrate high accuracy and reproducibility compared to the industry standard DNaseAlert™ . Finally, the entire detection system was implemented as a prototype device system utilizing single-use electrodes, custom-made cells, and electronics. The developed technology can improve nuclease quality control processes in the pharmaceutical/biotechnology industry and provide new insights into the importance of nucleases for medical applications.

1. Introduction

Nucleases are a family of hydrolytic enzymes that cleave phosphodiesteric bonds between nucleotides, producing 3′-phospho or 5′-phospho end products. These enzymes can be classified as endo- and exonucleases, cleaving at the inside of a polynucleotide chain or at the ends, respectively; however, some enzymes can show both activities (Yang, 2011). Typically, some nucleases prefer double-stranded nucleic acids (e.g., DNase I) (Suck, 1994), while others cleave single-stranded (e.g., nuclease P1) (Fujimoto et al., 1974) or RNA–DNA hybrid (RNase H) (Nakamura et al., 1991) polynucleotides. Deoxyribonucleases (DNases) are important targets in biotechnology and are used as tools for DNA manipulation (Pan et al., 2013) and appear as contaminants where nuclease-like activity is undesired (Senavirathne et al., 2015; Lopez et al., 2017). Furthermore, data have emerged indicating the importance of DNase activity detection for medical applications, i.e., DNases may be related to various diseases and could be used to monitor the progress of various cancers (Patel et al., 2000; Balian and Hernandez, 2021) and inflammatory diseases (Pedersen et al., 2018) as well as biomarkers for bacterial infections (Flenker et al., 2017). In a recent review by Balian and Hernandez it was shown that increased DNase I activity is related to gastric and colorectal carcinomas, and elevated activities of many other nucleases and cancers were demonstrated (Balian and Hernandez, 2021). Typically, DNases are being detected and quantified using a classical approach: fluorescence detection (Yonemura and Maeda, 1982; Choi and Szoka, 2000) or gel electrophoresis (Blank et al., 1982) techniques. Although these methods are highly sensitive and reliable, they are costly, time-consuming, and require toxic markers such as ethidium bromide or radiolabeled molecules (Vogel and Frantz, 2015; Boswell et al., 1989). As alternative methods, novel detection techniques for DNase detection have been reported, mainly based on fluorescence or chemiluminescence detection incorporating nanomaterials for signal enhancement (Mozioğlu et al., 2016; Gu et al., 2019; He et al., 2013). Electrochemical biosensors provide a simple and inexpensive platform

* Corresponding author. Life Sciences Center, Vilnius University, Saulėtekio al. 7, LT-10257 Vilnius, Lithuania.
E-mail address: Dalius.Ratautas@gmc.vu.lt (D. Ratautas).
[1] Both authors contributed equally.

https://doi.org/10.1016/j.bios.2022.114475
Received 14 April 2022; Received in revised form 5 June 2022; Accepted 8 June 2022
Available online 10 June 2022

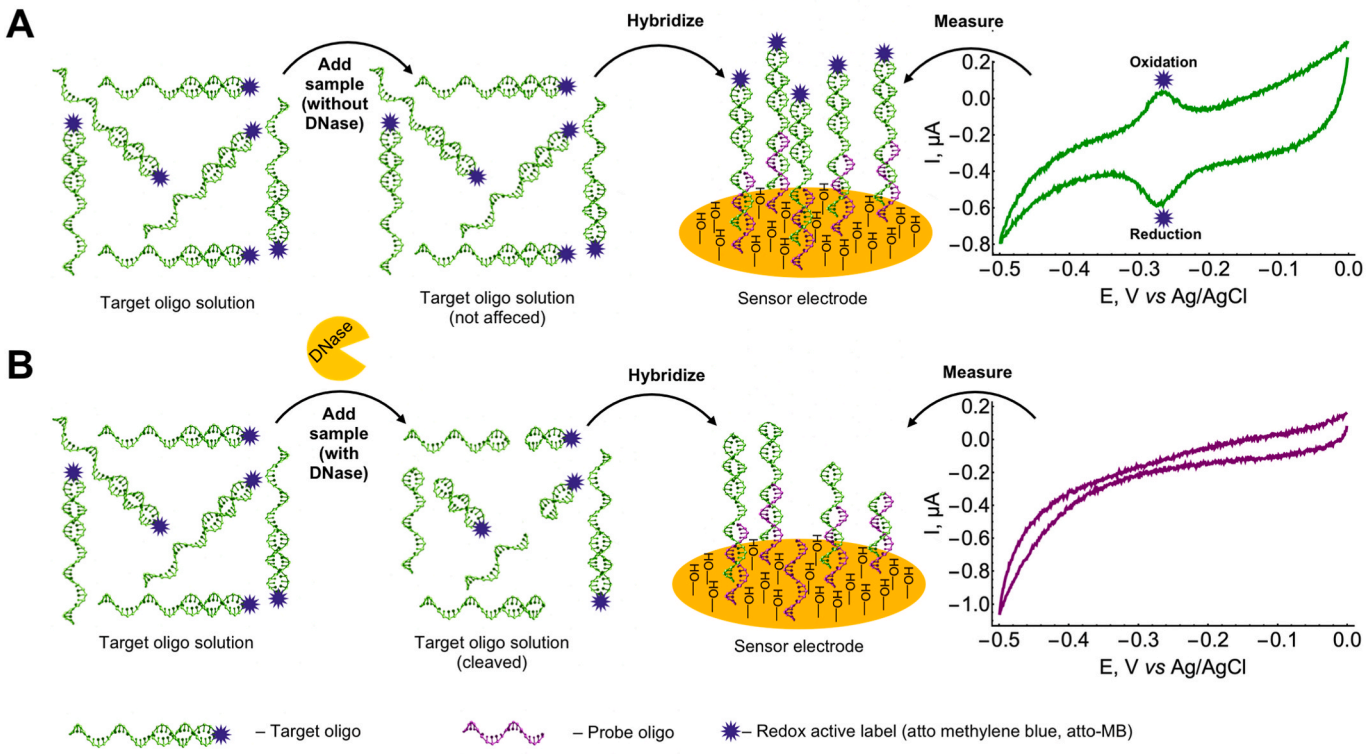

Fig. 1. The general operation scheme of the DNase biosensor. The target oligo is incubated with the sample. The hybridization rate between the target oligo and the sensor electrode is monitored. **(A)** The sample does not contain DNases. **(B)** The sample contains DNases.

for biomolecule detection while maintaining a high degree of accuracy and sensitivity. To date, the absolute majority of electrochemical biosensors have been developed for small biomolecules, e.g., glucose (Gineitytė et al., 2019; Ratautas and Dagys, 2019), glycerol (Ramonas et al., 2019), lactate (Yang et al., 1999), formaldehyde (Teišerskytė et al., 2021), and others. The targeting of large macromolecules, i.e., proteins or enzymes, is still somewhat lagging with a few exceptions (Agostini et al., 2021; Liu et al., 2022). Therefore, the development of electrochemical biosensors for these targets can produce novel sensitive assays. For the case of DNase detection, some biosensors have been reported. Sato et al. reported an electrochemical biosensor for DNase I detection based on ferrocene-modified DNA immobilized onto the electrode surface with a detection limit (LOD) of 10^{-2} U mL^{-1}. Ding and Qin reported a potentiometric biosensor for the detection of DNases based on a polycation-sensitive membrane, and for DNase I, a LOD of 0.45 U mL^{-1} was reported (Ding and Qin, 2013). Despite advances, electrochemical biosensors developed for DNase detection still lack sensitivities comparable to that of fluorescence or radiolabeling-based methods and the reliability required for the analysis of real samples.

In this work, we present a rapid and sensitive bioelectrochemical device for the determination of nuclease activity in various fluids which can significantly improve nuclease quality control processes in the pharmaceutical/biotechnology industry and provide new insights into the importance of nucleases for medical applications (Fig. 1).

2. Experimental

2.1. Materials and methods

DNase I (1000 U mL^{-1}, RNase-free), Ultra Low Range DNA Ladder (Invitrogen), TopVision Agarose Tablets, SYBR™ Gold Stain and DNaseAlert™ QC System were purchased from Thermo Fisher Scientific. Nuclease-free water, Tris(2-carboxyethyl)phosphine hydrochloride (TCEP), 6-mercapto-1-hexanol (MCH), and potassium hydroxide, and TBE buffer (89 mM Tris-borate and 2 mM EDTA, pH 8.3) were purchased from Sigma. Sodium dihydrogen phosphate and disodium hydrogen phosphate were purchased from Reachen Slovakia. Magnesium chloride hexahydrate, calcium chloride and sulfuric acid were purchased from Merck. Sodium chloride and Tris were obtained from Roth. All reagents were analytical grade. Nuclease-free water was used during the measurements.

Oligonucleotides were purchased from Metabion AG. The sequences are given in Table 1. The freeze-dried oligonucleotides obtained were dissolved in 10 mM Tris buffer solution, pH 8.00. The storage concentration of the probe sequence was 800 μM, and this solution was kept at −20 °C. The target oligo solution was prepared by heating a 10 mM Tris solution consisting of 40 μM DNA1 and 42 μM DNA2 sequences to 65 °C for 10 min and allowing the solution to cool down gradually. The probe oligo solution was prepared using TCEP solution (20 mM TCEP, 10 mM

Table 1
Oligonucleotides used in this research.

Oligonucleotide	Sequence (5' → 3')
Probe oligo	SH-C6-AATTATCAAACACAAACAGACTTAA
Target oligo	DNA1: GCCCGAGAGCAGTAGTCGTTAAGTCTGTTTGTGTTTGATAATT DNA2: CGACTACTGCTCTCGGGC-AttoMB
ssDNA oligo	AttoMB-GCCCGAGAGCAGTAGTCGTTAAGTCTGTTTGTGTTTGATAATT
Noncomplementary DNA oligo	AttoMB-CAGGTGGAACCTCATCAGGAGATGC

Tris, 100 mM $MgCl_2$, pH 7.2). This mixture was kept at room temperature in the dark for 1.0 h. After reduction, the oligonucleotides were diluted to a final concentration of 1.0 μM (10 mM Tris, 100 mM $MgCl_2$, pH 7.2). This solution was used to immobilize the probe oligo on the electrode surface and is referred to as the working probe solution (WPS).

2.2. Electrode preparation procedures

Gold disc (d = 2 mm) and screen-printed (d = 2 mm) electrodes for sensor preparation were purchased from BASi and Zimmer & Peacock, respectively. First, mechanical electrode cleaning was performed by rinsing the gold surface with deionized water and gently dabbing with lab tissue soaked with acetone. Subsequently, the electrodes were polished on microcloth wetted with deionized water and a 0.3 μm alumina suspension for several minutes, and mechanical cleaning was performed by sonicating the electrodes for 5 min in an ultrasound bath. Subsequently, electrochemical cleaning was performed, as described previously (Ratautas et al., 2017). Next, 2.0 μL of gold nanoparticle (AuNP) solution was placed onto the electrode surface and left to dry at room temperature. Once completely dry, the nanostructured surface was electrochemically cleaned once again. The prepared electrodes were placed into 120.0 μL WPS and kept at +4 °C overnight. Subsequently, the electrodes were thoroughly rinsed with deionized water, and submerged in 4.0 mM 6-mercapto-1-hexanol solution for 4 h at room temperature. Finally, the electrodes were stored in hybridization buffer (HBS, 20 mM PBS, 3M NaCl, pH 7.0) until measurements.

2.3. Preparation of samples

To obtain an artificial sample, 55.6 nM DNA oligonucleotide (either ssDNA, target or noncomplementary DNA oligo) was added to 3.5 mL of DNase I working buffer (DWB, 10 mM Tris-HCl, 2.5 mM $MgCl_2$, 0.5 mM $CaCl_2$, pH 7.6) solution. Afterward, a specific amount of DNase I was added. The solution was agitated at 37 °C for 30 min before being transferred to the electrochemical measurement cell.

Human saliva samples were purchased from UAB 'RDA Spot' (Lithuania). The samples were taken from volunteers under a written agreement. Saliva samples were collected from a volunteer into a sterile polypropylene tube. The collection was carried out in the morning before the volunteer ate or drank anything. The sample (800 μL) was centrifuged at 1600 rcf for 10 min and again at 16 000 rcf for 10 min. The supernatant (5.0 μL) was added to a 3.5 mL DWB solution containing 55.6 nM target oligo. The solution was gently mixed by inverting, and the reaction was carried out at 37 °C for 30 min with agitation. Finally, the resulting solution was measured using cyclic voltammetry.

2.4. Methods

Electrochemical measurements were conducted in a 7.0 mL cell using a three-electrode system (probe oligo-modified working electrode, Pt auxiliary electrode, and Ag/AgCl (3 M KCl) reference electrode) with a Gamry Reference 600™ potentiostat. The experiments were carried out in a 1:1 (V/V) mixture of HBS and sample solutions at 45 °C. The cell was constantly stirred between cyclic voltammetry (CV) measurements, but the stirring was turned off while the CVs were being recorded. CVs were run from 0 to −0.5 V at a scan rate of 0.05 V s^{-1}. CVs were recorded at intervals of 1 min, 5 min, or 10 min. Electrochemical measurements with single-use electrodes followed the same protocol, except that the stirring was not turned off even when the CVs were being recorded.

DNA electrophoresis was conducted to investigate the cleavage of double-stranded DNA (target oligo) and single-stranded DNA (ssDNA oligo) oligonucleotides. The target and ssDNA oligo solutions (26.6 μM in DWB) were incubated with DNase I at 36 °C (0 U mL^{-1} for the control and 2.6 U mL^{-1} for the test). Subsequently, the oligonucleotide solutions were diluted with an equivalent volume of DNase I inhibition solution (200 mM EDTA, 1.5 M Na_2HPO_4, pH 7) and mixed. Agarose gel (5.0%) was loaded with a ladder (3.0 μl per lane) and the electrophoresis was performed of eight samples (10.0 μl per lane) in TBE buffer at 80 V for 80 min. The gel was submerged in a water bath to prevent an increase in the buffer solution temperature. Next, the gel was stained with SYBR Gold in TBE for 1 h.

DNase Alert™ sample testing was carried out using the manufacturer's instructions with a PerkinElmer LS fluorescence spectrometer equipped with a biokinetic accessory and a thermostat. Briefly, 315 μL of nuclease-free water was mixed with 45 μL 10X NucleaseAlert buffer, 45 μL DNase Alert Substrate, and 45 μL of saliva supernatant. The solution

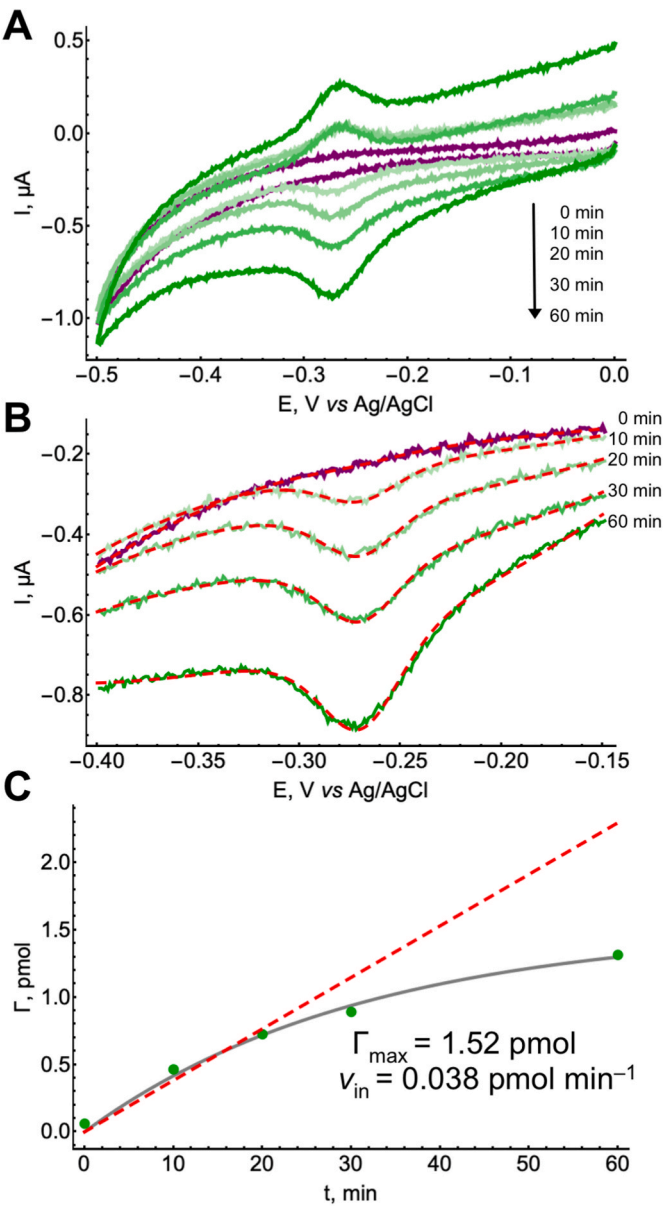

Fig. 2. Electrochemical analysis of the sensor electrode demonstrating the hybridization of ssDNA oligo with atto-MB. **(A)** CV analysis of the electrode after the addition of a 60 nM ssDNA oligo. CVs were recorded at different times after addition of ssDNA oligo in the range 0–60 min. **(B)** The fitting of cathodic current values to the model (SI, Equation S(1)). Green data points indicate the measurement data, while red dashed lines indicate fitted curves with surface coverage values. **(C)** Curve demonstrating the dependence of the hybridization of ssDNA oligo on time. Surface coverage values were fitted to a model (SI, Equation S(1)), and the hybridization parameters were extracted. The red dotted line demonstrates the fit of the initial hybridization data to a linear model.

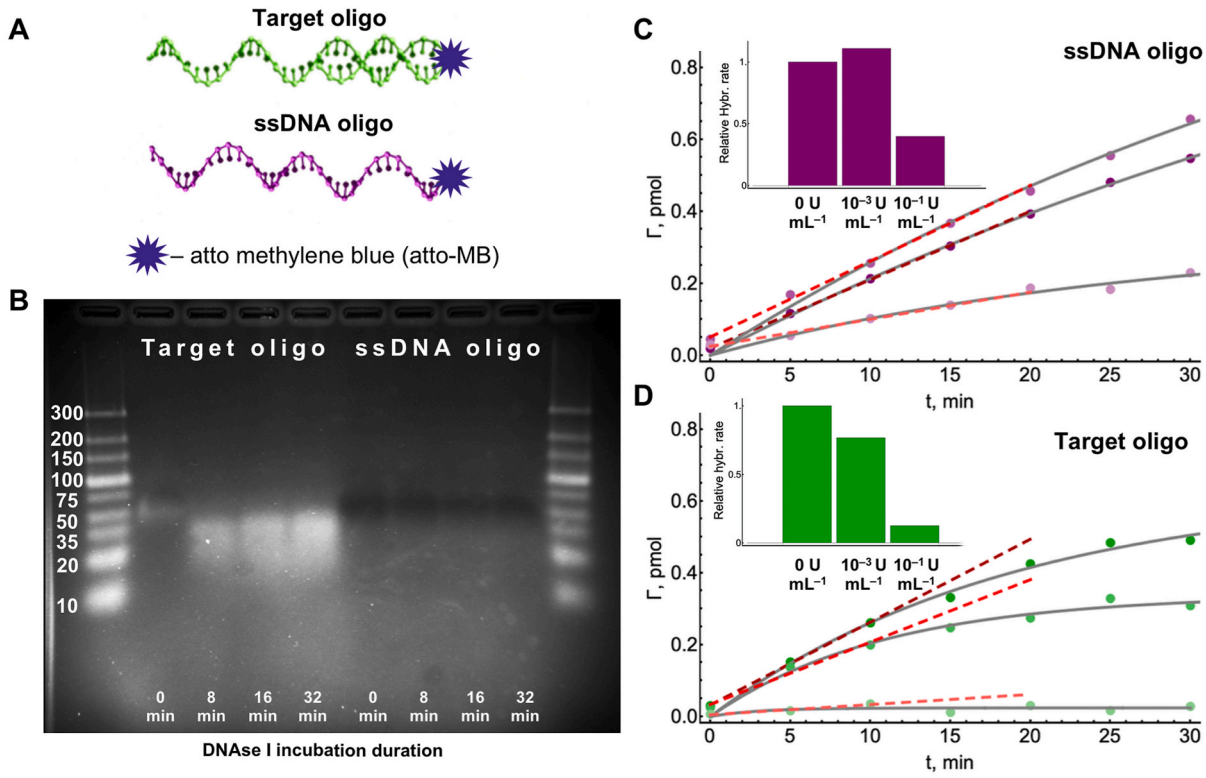

Fig. 3. Comparison of DNase I activity for single-stranded DNA (ssDNA oligo) and hybrid (containing both single- and double-stranded) DNA (target oligo). **(A)** Schematic illustration of DNA oligonucleotides used to investigate DNase I activity – ssDNA oligo (purple) and target oligo (green). **(B)** Gel electrophoresis for the target (lanes 1–4) and ssDNA oligos (lanes 5–8). The lane progresses by increasing the incubation time with DNase I (0 min, 8 min, 16 min, 32 min). **(C)** Curve demonstrating the hybridization rate of ssDNA oligos incubated with solutions of various DNase I activities. The inset shows the relative hybridization rate dependence on DNase I solution activity. **(D)** Curve demonstrating the hybridization rate of the target oligo incubated with solutions of various DNase I activities. The inset shows the relative hybridization rate dependence on DNase I solution activity.

was measured in a low volume quartz cuvette with stirring at 37 °C using real-time fluorescence measurements at 30 s intervals (Ex: 535 nm, Em: 556 nm).

3. Results and discussion

3.1. Development of DNA-modified electrodes for DNA hybridization

Designing an electrode surface capable of hybridizing DNA at high rates and specificities was critical for a functioning nuclease sensor. The final iteration electrodes, prepared using AuNPs, with immobilized probe oligo (Table 1) and self-assembled MCH monolayer, were named sensor electrodes. The representation of the sensor electrode is presented in Fig. 1. The rationale for using AuNPs is based on our previous experience indicating that AuNPs significantly increase the active surface area of the electrode and allow for the adsorption of more biomolecules (Ratautas et al., 2016). MCH was used based on previous works, which have shown that self-assembled monolayers significantly improve the efficiency and specificity of DNA immobilization on gold (Steel et al., 1998; Lao et al., 2005; Farjami et al., 2010, 2012).

The sensor electrode was used to investigate the hybridization parameters of the complementary ssDNA oligo with the redox-active marker (atto-MB) at the 3' end. After the addition of the ssDNA oligo, the CVs were recorded from 0 to −0.5 V after 0–60 min (Fig. 2A). CV analysis did not show a significant electrochemical process immediately after the addition of ssDNA oligo (t = 0 min, purple curve). After 10 min, CV was recorded again, and atto-MB reduction and oxidation peaks were observed at −0.271 V and −0.265 V, respectively. These potential values were found to be similar to that for methylene blue redox on DNA-modified electrodes, as reported previously (Kelley et al., 1997). The electrode was allowed to hybridize for up to 60 min, while the CVs were recorded at 20, 30 and 60 min. CVs demonstrate an increase in current values, but no significant changes in potentials are observed, thus providing evidence for the progression of DNA hybridization on the electrode. It is important to note that the potential difference between the cathodic and anodic peaks is only 0.006 V, showing the electrochemistry of surface-bound species (Bard and Faulkner, 2001). Control experiments were carried out to demonstrate that specific DNA–DNA hybridization is observed (SI, Figs. S2–S5). Controls were recorded using electrodes without probe oligo, without MCH and using the final sensor electrode (both MCH and probe oligo) but adding a noncomplementary DNA oligo. In all three cases, no increase in redox peaks was observed.

We investigated the kinetics of ssDNA oligo hybridization to evaluate its surface coverage and rate. First, we estimated the amount of ssDNA oligo on the electrode surface by fitting the CV data to the potential-current function for surface-adsorbed redox-active species from Bard (Bard and Faulkner, 2001) (SI, 1. Fitting). The fitting was carried out for a cathodic scan in the potential range of −0.15 to −0.4 V (Fig. 2 B; SI, Equation S(1)) and demonstrated excellent agreement with the experimental data points. From the fitted CV curves, the molar number for the ssDNA oligo was determined to vary in the range of 0–1.2 pmol. Afterward, we evaluated the hybridization rate and the surface saturation of the sensor electrode with the ssDNA oligo (Fig. 2C). Molar numbers of ssDNA oligo were plotted against time and fitted to the equation describing time-dependent DNA hybridization on the electrode (SI, Fitting, Equation S(2)). The data show excellent agreement with the experimental results, indicating that DNA hybridization on the electrode can be approximated using first-order kinetics. The maximum molar number for hybridized ssDNA oligo is approximately 1.5 pmol (or calculated to be 75 pmol cm^{-2} for a geometric electrode surface area).

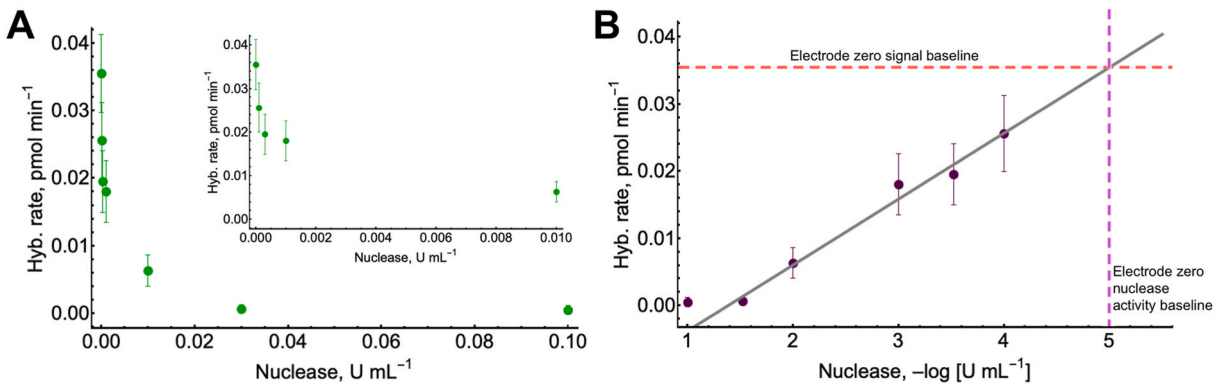

Fig. 4. The sensor electrode performance when hybridized with 55.6 nM target oligo solutions incubated with various DNase I activities (0, 10^{-4}, 3×10^{-4}, 10^{-3}, 10^{-2}, 3×10^{-2}, 10^{-1} U mL^{-1}). **(A)** Dependence of the hybridization rate on DNase activity (0–10^{-1} U mL^{-1}). The inset shows a lower DNase activity range (0–10^{-2} U mL^{-1}). **(B)** Calibration curve demonstrating a linear dependence on the negative logarithm of nuclease activity.

This number is much higher than the values reported previously (1.6–6.5 pmol cm^{-2}) (Steel et al., 1998; Zhang et al., 2007) and can be attributed to the usage of gold nanoparticles, which significantly increase the surface area and allow more complementary DNA to hybridize. To evaluate the hybridization rate, the initial data points (up to 15 min) were fitted to a linear model (Fig. 2C, red line), and the slope of the line was named v_{in}. The value of v_{in} shows the hybridization rate (pmol min^{-1}) and can be further used in the developed biosensor to evaluate the nuclease activity.

3.2. Optimization of the DNA oligonucleotide for maximum and nonspecific DNase activity

Once we have developed an electrode for fast and selective hybridization of DNA and a method to evaluate the hybridization rate, a DNA target sensitive to a broad nuclease activity is required. DNases have sequence-dependent activity, most notably significant activity differences for single- and double-stranded DNA (Suck, 1994; Dingwall et al., 1981; Desai and Shankar, 2003). Our aim was to detect total nuclease activity in a sample, thus indiscriminately detecting the activity of most nucleases. For this reason, we designed a hybrid DNA oligonucleotide composed of single- and double-stranded DNA (Fig. 3A). This oligonucleotide is composed of longer (43 nt) and shorter (18 nt) DNA chains hybridized together in a solution and was named the target oligo. Initially, electrophoresis was conducted to investigate the activity of the model enzyme DNase I toward ssDNA and target oligos (Fig. 3B). The results demonstrate that the target and ssDNA oligos are bound to the SYBR Gold dye, which emits at a wavelength of ~537 nm, while the redox-active label atto-MB absorbs light at ~668 nm. As a result, darker bands are visible on the gel with atto-MB-labeled oligos, indicating that the fragments are not affected by nucleases (t = 0 min). Significant differences between the target and ssDNA oligos appear after 8–32 min of incubation with DNase I. Broader bright bands appear as the target oligo is cleaved by DNase I, since the redox-active label atto-MB is removed from the DNA chain. In contrast, the ssDNA oligo did not show any obvious signs of a decrease in mass or band broadening, indicating that this type of DNA is not significantly affected by DNase I.

Electrochemical measurements show that both the ssDNA and target oligos are able to hybridize with the probe oligo attached to the surface and approach the surface saturation (Fig. 3CD). CV measurements were carried out using oligos treated with DNase I solution with different activities (0, 10^{-3}, 10^{-1} U mL^{-1}) (Fig. 3CD). The results demonstrate that the target oligo shows an apparent decrease in the hybridization rate (v_{in}) with an increase in DNase I activity (Fig. 3D, inset). The hybridization rate of the ssDNA oligo is only decreased at significantly higher DNase I activities. Thus, a custom-designed target oligo was chosen as a nucleotide for DNase detection.

3.3. Characterization and performance of the nuclease activity biosensor, prototype biosensor development

The sensor electrodes were calibrated using DNase I solutions with various activities. First, the target oligo was incubated with 0–10^{-1} U mL^{-1} DNase I and then hybridized with the sensor electrodes. The dependence of the hybridization rate (v_{in}) on the nuclease activity is presented in Fig. 4. The data show that v_{in} for the target oligo is related to nuclease activity. For the case when no DNase I is used, v_{in} is 0.035 ± 0.005 pmol min^{-1}. For example, when the target oligo is incubated with 10^{-1} U mL^{-1} DNase I, v_{in} is decreased to 0.00047 ± 0.0007 pmol min^{-1}. To carry out the calibration, we plotted the dependence of the hybridization rate against the negative logarithm of nuclease activity (Fig. 4B). The data were fitted to a linear model, and a calibration curve was obtained:

$$y = -\log[Nuclease]a + b \quad \text{(Equation 1)}$$

Here, a – slope (0.0098), b – intercept (0.014). It is important to determine the parameters of the biosensor, the limit of detection (LOD) and the sensitivity. Sensitivity is usually defined as the slope of the calibration curve (Bhalla et al., 2016); therefore, the sensitivity of the biosensor was determined to be 0.0098 pmol min^{-1} (–log[nuclease activity])$^{-1}$, with the biosensor showing that a 10-fold increase in nuclease activity results in a 2-fold change in signal. LOD is typically estimated using the 3 σ criterion and is defined as LOD = 3 σ of the signal blank/sensitivity corresponding to a confidence level of 99.7% (Lavín et al., 2018). Since there is no standardized method to define the LOD for a negative signal sensor, we determined the LOD using the 3 σ criterion and additionally evaluated the electrode zero-nuclease activity baseline (purple curve in Fig. 4B). Thus, LOD = electrode zero-nuclease activity baseline – 3 σ of the electrode zero signal baseline/sensitivity. The calculations gave an LOD value of 3.47, which is equal to 3.4×10^{-4} U mL^{-1}. The lowest nuclease activity point in calibration (10^{-4} U mL^{-1}) is lower than the calculated LOD; however, we emphasize that we present the LOD based on a confidence level of 99.7% (3 σ). For this reason, high reliability can only be achieved when measuring in the range 3.4×10^{-4} to 3×10^{-2} U mL^{-1}. A detailed comparison between our developed sensor and other relevant works is presented in SI, Table S1.

To demonstrate the practical application of the system, we built a biosensor prototype system. The prototype was built around a customized PTFE electrochemical cell, which was integrated into a Peltier element-based thermostatic cell system with a magnetic stirrer. The electronic system was developed using an Arduino Due electronic set linked with a laptop computer *via* a USB interface. The biosensor prototype was tested under various nuclease concentrations and found to give reproducible results (SI, 4. Biosensor prototype system).

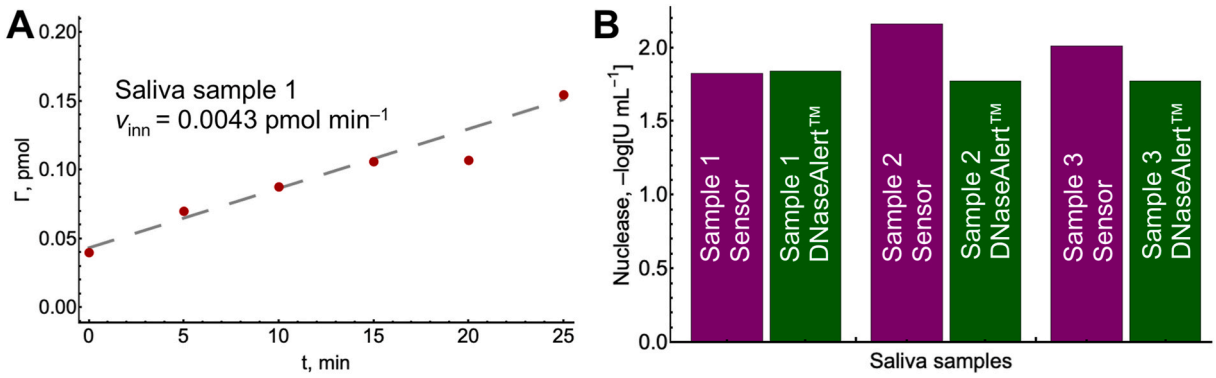

Fig. 5. DNase activity determination in human saliva samples taken from the same subject. **(A)** Time-dependent target oligo hybridization after incubation with human saliva samples. **(B)** A comparative histogram demonstrating nuclease activity in human saliva samples measured with the developed sensor and compared with the industry standard DNaseAlert™ .

3.4. DNase activity determination in human saliva samples

To show that operation with biological fluids is possible we measured nuclease activity in human saliva samples. The target oligo was incubated with saliva samples and subsequently hybridized on the sensor electrodes. The typical hybridization is presented in Fig. 5A. The hybridization line shows that the target oligo after incubation with saliva sample is capable of hybridizing but at a significantly lower rate; for example, for sample 1, v_{in} is equal to 0.00432 pmol min^{-1}. Using the calibration curve (Equation (1)), the hybridization rates were converted to DNase activity, and considering a sample dilution, the nuclease activities were calculated to vary in the range of 6.5–10.6 U mL^{-1}. Additionally, we used DNaseAlert™ to analyze the saliva samples. A comparison of the results obtained with the Sensor and DNaseAlert™ is presented in Fig. 5B. The results demonstrate that the sensor electrodes give results that are comparable with an alternative method. It can be observed that the logarithmic difference in nuclease activity between the Sensor electrodes and DNaseAlert™ varies in the range of 1–18%. The absolute difference in nuclease activity is presented in SI, Table S1 and varies in the range of 4–81%. The difference in nuclease activity measurements between our method and DNaseAlert™ most likely risen due to differences in the DNA substrate sequence resulting in somewhat different affinities towards DNases.

4. Conclusions

In this paper, we report a new bioelectrochemical device – a rapid and sensitive nuclease detection system consisting of a sensor electrode, a custom-designed DNA oligonucleotide target to maximize the nuclease cleavage rate, a signal analysis algorithm, and supporting electronics. Our designed sensor electrode is prepared by immobilizing gold nanoparticles on a gold electrode after immobilization of the DNA probe with the supporting layer (6-mercapto-1-hexanol) to form a specific DNA surface with a high DNA surface coverage of 1.5 pmol (or calculated as 75 pmol cm^{-2} for a geometric electrode surface area). The sensor electrode is capable of hybridizing a redox-labeled complementary DNA with a high rate (up to 0.04 pmol min^{-1}) and selectivity. We also designed a custom DNA oligonucleotide for the detection and monitoring of DNase activity. The DNA oligonucleotide is composed of both single- and double-stranded DNA to ensure the suitability of the oligonucleotide for various types of nucleases and is additionally labeled with atto methylene blue (atto-MB) for electrochemical detection. The hybridization of DNA oligonucleotide with atto-MB was monitored and fitted to a potential-current function to determine the rate of hybridization. The nuclease-treated DNA oligonucleotide was cleaved, thus resulting in a lower rate of hybridization, and, in turn, lower development of the signal. The designed biosensor enabled us to determine DNase activity in the range of 3.4×10^{-4} to 3×10^{-2} U mL^{-1} with a detection limit of 3.4×10^{-4} U mL^{-1}. Furthermore, the sensor was tested by measuring nuclease activity in human saliva samples and was found to demonstrate high accuracy and reproducibility compared to the industry standard DNaseAlert™. Finally, the whole system was implemented in the design of a prototype biosensor excluding the standard laboratory equipment (e.g., cells, thermostats, potentiostats). The device contained a custom polytetrafluoroethylene (PTFE) reaction cell, the electronic part, and a program written in Python language for electrochemical signal analysis and data fitting.

Funding

This research was funded by Agency for Science, Innovation and Technology (Lithuania) under the measure of "Development of biotechnology industry in Lithuania" grant no: BIOTECH-02-005.

CRediT authorship contribution statement

Skomantas Serapinas: Conceptualization, Software, Investigation, Methodology, Formal analysis, Data curation, Validation, Writing – review & editing. **Justina Gineitytė:** Conceptualization, Software, Investigation, Methodology, Formal analysis, Data curation, Validation, Writing – review & editing. **Marius Butkevičius:** Conceptualization, Software, Investigation, Methodology, Formal analysis, Writing – review & editing. **Rapolas Danilevičius:** Conceptualization, Writing – review & editing, Resources. **Marius Dagys:** Conceptualization, Software, Methodology, Writing – review & editing, Resources. **Dalius Ratautas:** Conceptualization, Methodology, Software, Formal analysis, Writing – original draft, Writing – review & editing, Visualization, Resources, Supervision.

Declaration of competing interest

The authors declare that they have no known competing financial interests or personal relationships that could have appeared to influence the work reported in this paper.

Appendix A. Supplementary data

Supplementary data to this article can be found online at https://doi.org/10.1016/j.bios.2022.114475.

References

Agostini, M., Amato, F., Vieri, M.L., Greco, G., Tonazzini, I., Baroncelli, L., Caleo, M., Vannini, E., Santi, M., Signore, G., Cecchini, M., 2021. Biosens. Bioelectron. 172, 112774 https://doi.org/10.1016/j.bios.2020.112774.

Balian, A., Hernandez, F.J., 2021. Biomarker Research 9, 86. https://doi.org/10.1186/s40364-021-00342-4.
Bard, A.J., Faulkner, L.R., 2001. Electrochemical Methods: Fundamentals and Applications, second ed. Wiley, New York.
Bhalla, N., Jolly, P., Formisano, N., Estrela, P., 2016. Essays Biochem. 60, 1–8. https://doi.org/10.1042/EBC20150001.
Blank, A., Sugiyama, R.H., Dekker, C.A., 1982. Anal. Biochem. 120, 267–275. https://doi.org/10.1016/0003-2697(82)90347-5.
Boswell, G.S., Dimitrijevich, S.D., Gracy, R.W., 1989. Anal. Biochem. 182, 20–24. https://doi.org/10.1016/0003-2697(89)90711-2.
Choi, S.-J., Szoka, F.C., 2000. Anal. Biochem. 281, 95–97. https://doi.org/10.1006/abio.2000.4529.
Desai, N.A., Shankar, V., 2003. FEMS (Fed. Eur. Microbiol. Soc.) Microbiol. Rev. 26, 457–491. https://doi.org/10.1111/j.1574-6976.2003.tb00626.x.
Ding, J., Qin, W., 2013. Biosens. Bioelectron. 47, 559–565. https://doi.org/10.1016/j.bios.2013.03.066.
Dingwall, C., Lomonossoff, G.P., Laskey, R.A., 1981. Nucleic Acids Res. 9, 2659–2674. https://doi.org/10.1093/nar/9.12.2659.
Farjami, E., Campos, R., Ferapontova, E.E., 2012. Langmuir 28, 16218–16226. https://doi.org/10.1021/la3032336.
Farjami, E., Clima, L., Gothelf, K.V., Ferapontova, E.E., 2010. Analyst 135, 1443. https://doi.org/10.1039/c0an00049c.
Flenker, K.S., Burghardt, E.L., Dutta, N., Burns, W.J., Grover, J.M., Kenkel, E.J., Weaver, T.M., Mills, J., Kim, H., Huang, L., Owczarzy, R., Musselman, C.A., Behlke, M.A., Ford, B., McNamara, J.O., 2017. Mol. Ther. 25, 1353–1362. https://doi.org/10.1016/j.ymthe.2017.03.015.
Fujimoto, M., Kuninaka, A., Yoshino, H., 1974. Agric. Biol. Chem. 38, 1555–1561. https://doi.org/10.1080/00021369.1974.10861384.
Gineitytė, J., Meškys, R., Dagys, M., Ratautas, D., 2019. J. Power Sources 441, 227163. https://doi.org/10.1016/j.jpowsour.2019.227163.
Gu, Z., Fu, A., Ye, L., Kuerban, K., Wang, Y., Cao, Z., 2019. ACS Sens. 4, 2922–2929. https://doi.org/10.1021/acssensors.9b01303.
He, Y., Xiong, L.-H., Xing, X.-J., Tang, H.-W., Pang, D.-W., 2013. Biosens. Bioelectron. 42, 467–473. https://doi.org/10.1016/j.bios.2012.10.045.
Kelley, S.O., Barton, J.K., Jackson, N.M., Hill, M.G., 1997. Bioconjugate Chem. 8, 31–37. https://doi.org/10.1021/bc960070o.
Lao, R., Song, S., Wu, H., Wang, L., Zhang, Z., He, L., Fan, C., 2005. Anal. Chem. 77, 6475–6480. https://doi.org/10.1021/ac050911x.
Lavín, Á., Vicente, J., Holgado, M., Laguna, M., Casquel, R., Santamaría, B., Maigler, M., Hernández, A., Ramírez, Y., 2018. Sensors 18, 2038. https://doi.org/10.3390/s18072038.
Liu, N., Liu, R., Zhang, J., 2022. Bioelectrochemistry 146, 108105. https://doi.org/10.1016/j.bioelechem.2022.108105.
Lopez, M.A., Mackler, R.M., Altman, M.P., Yoder, K.E., 2017. JoVE 130, e56605. https://doi.org/10.3791/56605.
Mozioğlu, E., Akgoz, M., Kocagöz, T., Tamerler, C., 2016. Anal. Methods 8, 4017–4021. https://doi.org/10.1039/C5AY02310F.
Nakamura, H., Oda, Y., Iwai, S., Inoue, H., Ohtsuka, E., Kanaya, S., Kimura, S., Katsuda, C., Katayanagi, K., Morikawa, K., 1991. Proc. Natl. Acad. Sci. USA 88, 11535–11539. https://doi.org/10.1073/pnas.88.24.11535.
Pan, Y., Xiao, L., Li, A.S.S., Zhang, X., Sirois, P., Zhang, J., Li, K., 2013. Mol. Biotechnol. 55, 54–62. https://doi.org/10.1007/s12033-012-9613-9.
Patel, P.S., Patel, B.P., Rawal, R.M., Raval, G.N., Patel, M.M., Patel, J.B., Jha, F.P., Patel, D.D., 2000. Tumor Biol. 21, 82–89. https://doi.org/10.1159/000030113.
Pedersen, H.L., Horvei, K.D., Thiyagarajan, D., Norby, G.E., Seredkina, N., Moroni, G., Eilertsen, G.Ø., Holdaas, H., Strøm, E.H., Bakland, G., Meroni, P.-L., Rekvig, O.P., 2018. J. Pathol.: Clin. Res. 4, 193–203. https://doi.org/10.1002/cjp2.99.
Ramonas, E., Ratautas, D., Dagys, M., Meškys, R., Kulys, J., 2019. Talanta 200, 333–339. https://doi.org/10.1016/j.talanta.2019.03.063.
Ratautas, D., Dagys, M., 2019. Catalysts 10, 9. https://doi.org/10.3390/catal10010009.
Ratautas, D., Laurynėnas, A., Dagys, M., Marcinkevičienė, L., Meškys, R., Kulys, J., 2016. Electrochim. Acta 199, 254–260. https://doi.org/10.1016/j.electacta.2016.03.087.
Ratautas, D., Tetianec, L., Marcinkevičienė, L., Meškys, R., Kulys, J., 2017. Biosens. Bioelectron. 98, 215–221. https://doi.org/10.1016/j.bios.2017.06.048.
Senavirathne, G., Liu, J., Lopez, M.A., Hanne, J., Martin-Lopez, J., Lee, J.-B., Yoder, K.E., Fishel, R., 2015. Nat. Methods 12, 901–902. https://doi.org/10.1038/nmeth.3588.
Steel, A.B., Herne, T.M., Tarlov, M.J., 1998. Anal. Chem. 70, 4670–4677. https://doi.org/10.1021/ac980037q.
Suck, D., 1994. J. Mol. Recogn. 7, 65–70. https://doi.org/10.1002/jmr.300070203.
Teišerskytė, V., Urbonavičius, J., Ratautas, D., 2021. Talanta 234, 122657. https://doi.org/10.1016/j.talanta.2021.122657.
Vogel, B., Frantz, S., 2015. Anal. Biochem. 471, 73–79. https://doi.org/10.1016/j.ab.2014.11.013.
Yang, Q., Atanasov, P., Wilkins, E., 1999. Biosens. Bioelectron. 14, 203–210. https://doi.org/10.1016/S0956-5663(98)00109-2.
Yang, W., 2011. Q. Rev. Biophys. 44, 1–93. https://doi.org/10.1017/S0033583510000181.
Yonemura, K., Maeda, H., 1982. J. Biochem. 92, 1297–1303. https://doi.org/10.1093/oxfordjournals.jbchem.a134048.
Zhang, J., Wang, L., Pan, D., Song, S., Fan, C., 2007. Chem. Commun. 1154–1156. https://doi.org/10.1039/B615742D.